

Senior Brigadier, Prof., PhD., Eng. Zoja BEDNAREK

The Main School of Fire Service, Warszawa

PhD., MSc. Eng. Marek SKŁODOWSKI

Institute of Fundamental Technological Research, PAN, Warszawa

TESTING OF SOFT SELF-SUPPORTING WATER TANK USED FOR FIRE PROTECTION OF CIVIL STRUCTURES

Investigated flexible self supporting water tank is made of fibre reinforced rubber and can be used in fire-extinguishing actions to protect buildings and other civil engineering structures. Its self supporting ability results from the air-tight floating flange. Preliminary investigations of the rubber material done in the laboratory and of a prototype tank led to the tank redesign. Deformations of a new tank were measured under its operating conditions with four tons of water inside. Resulting hoop and longitudinal strains exceed four percent and are in agreement with theoretical considerations. Developed measurement methods can be adapted for testing the shell structures and other coverings made of technical fabrics.

Testowany elastyczny, samonośny zbiornik na wodę wykonany jest z gumy wzmocnionej włóknami i może być użyty w akcjach gaśniczych w celu ochrony budynków i innych obiektów cywilnych. Jego samonośna zdolność wynika ze szczelnego samonośnego kołnierza. Wstępne badania materiałowe gumy przeprowadzone w laboratorium, jak i badania prototypu zbiornika doprowadziły do zmian w jego projekcie. Dokonano pomiarów odkształceń w nowym zbiorniku, zawierającym 4 tony wody, w warunkach prowadzenia akcji. Powstałe obwodowe, jak i wzdłużne odkształcenia przekraczają 4% i zgadzają się z teoretycznymi założeniami. Opracowane metody pomiarów mogą być wykorzystane do testowania konstrukcji łupinowych oraz innych pokryć wykonanych z włókien technicznych.

1. Introduction

Temporary water tanks of a volume from a few to several cubic meters are often used by firefighters during the extinguishing action. One obvious feature of such a tank is its water tightness which should be followed by short operational readiness, light weight and small storage volume. Tanks with flexible walls supported on a frame structure (Fig. 1) have been used for many years although they have been far from optimal solution.

Flexible self-supporting water tank (FST) is much easier to operate (as shown in Fig. 1b, c, d) and has much more advantages than the old ones. The study of a mechanical behaviour of the FST was the part of the research performed under the support of State Committee for Scientific Research and in the paper presents measurements of deformations of the FST walls of two tanks.

First one is the prototype tank and the other is modified after the preliminary research. In both cases nominal operating conditions are concerned i.e. tanks are filled with 4 m³ of water.



Fig. 1. Supported on a frame (a) and new self-supporting (b, c, d) water tanks

2. Tested water tanks

2.1. Material properties

A research carried [1] on several rubberised woven materials showed that TU-08 rubberised fabric produced by STOMIL is a suitable material for FST manufacturing [1].

The research showed that TU - 08 has various strength and deformation properties if loaded in the weft and warp directions:

ultimate strength in warp direction 11.14 daN/mm²;

ultimate strength in weft direction 9.89 daN/mm²;

secant elasticity modulus (average for stresses from 0 to ultimate strength):

$E_{s_{warp}} = 59.6 + -2.5$ daN/mm²;

$E_{s_{weft}} = 35.6 + -1.4$ daN/mm²;

material thickness $t = 0.72$ mm.

Its typical load-displacement characteristic under uniaxial tension is shown in Fig. 2.

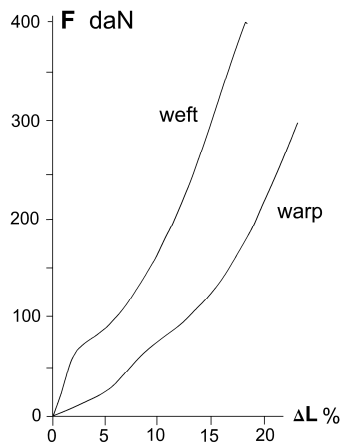


Fig. 2. Load-displacement characteristic of TU – 08 rubbered fabric in warp and weft directions – after [1]

2.2. FST design

Side walls of a flexible self-supporting water tank are made of 4 curve-linear trapezoid gores glued together into a shape of a truncated circular cone. The base of the tank is made of gores glued together as well as to the side walls. All joints are strengthened with belts glued over them. This results in local variation of the tank wall thickness from 0.72 mm to over 6 mm in case of cross joints of vertical and horizontal belts. The greatest thickness and stiffness of the FST is the vicinity of the quick-closing valve at the bottom of the tank. Upper edges of the side walls are glued to the air-chamber tuber which forms a floating flange of the tank. Geometry of the prototype and final test copy of the FST are given in Fig. 3.

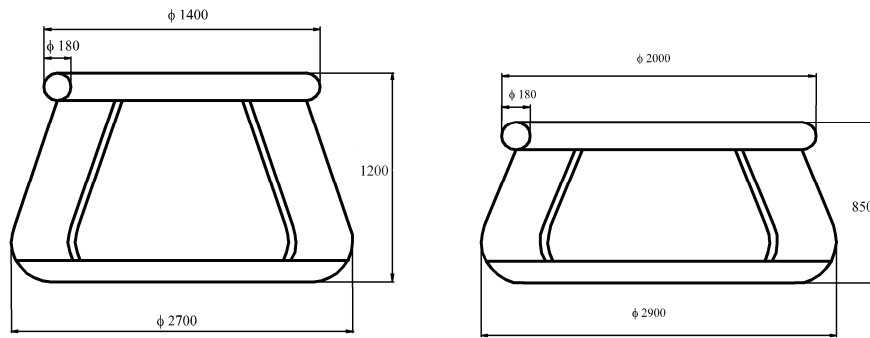


Fig. 3. Prototype and final test copy of FST

2.3. Estimated strains and range of the measurement method

Calculation of expected strains was done prior to experiments in order to find a measurement range and help to choose the appropriate measurement methods. Following data and assumptions form the basis of the strain estimation in the prototype FST:

- hydrostatic pressure of water stored in the tank is the only load applied to the tank (thus e.g. weight of the structure, side wind pressure, non flatness of the ground beneath the FST base are neglected);
- side walls are of the cylindrical shape (which means that vertical shape variation due to the conical design and linear pressure distribution are neglected and constant wall thickness with no joints and gores is assumed);
- elastic moduli are equal to the average secant moduli of elasticity given in 2.2.

Taking into account the dimensions of the prototype FST shown in Fig. 3 one gets estimated circumferential stress in a lower part of the tank

$$\sigma_{1\max} = pd_{\max}/2t \cong 1.875 \text{ daN/mm}^2,$$

$$\varepsilon_{1\text{warp}} = \sigma_{1\max} / Es \cong 3.1\% \text{ or}$$

$$\varepsilon_{1\text{warp}} = \sigma_{1\max} / Es_{\text{weft}} \cong 5.3\%$$

depending on the orientation of the laminated fabric of gores (which was unknown). Accounting for the second curvature of the wall near FST base results in a conclusion that it can only diminish the stresses and strains of the wall. Similarly the vertical stresses introduced by the floating air flange are many times lower than the estimated σ_{\max} . On the other hand one can expect that the stress concentration may arise near the groves connection lines due to the local changes of the wall thickness. Thus the expected strain measurement range can be evaluated as

$$\text{(at the top)} \quad 0\% \leq \varepsilon \leq 7-8\% \quad \text{(at the bottom).}$$

3. Experiments

Laboratory research was carried on to find out measurement methods suitable for further in-situ investigations [2]. For this purpose, the results of displacement/strain measurements for uniaxial tensile test of the 70 mm × 256 mm specimen of TU - 08 rubberised fabric with load applied in the weft direction were compared. After the application of the preliminary load of 35 daN the specimen was unloaded to 25 daN and the measurements were taken under this condition which results in an average tensile stress 0.5 daN/mm². The load was applied eight times and so were taken the measurements with resistant strain gauges, strain gauge extensometer, texture photography, grid sensor and digital displacement caliper. Strain gauge extensometer shown schematically in Fig. 4 has four strain gauges on its two flexible arms and can be attached to the FST by introducing the end pins into the hollow cylindrical grips glued to the fabric surface.

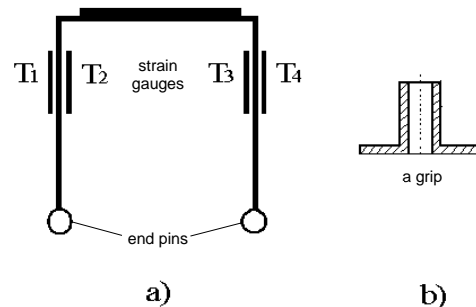


Fig. 4. A sketch of the strain gauge extensometer

The sensor is easily removable and can be used for sequential measurements in various points during the same experiment. To take texture images before and after the loading of the specimen, the non-contact texture photography was used. The processed film was illuminated with point-wise laser beam and the transmitted light with a diffraction lines was projected onto a screen. Measuring the distance between the diffraction fringes in the unloaded (d_0) and loaded (d_1) states one can calculate the strain as $\varepsilon = \frac{d_1}{d_0} - 1$.

The grid sensor was designed especially for the purpose of the low cost large strain in-situ measurement. As it is shown in Fig. 5 it consists of two separate strips with printed line sets. One set has line spacing 1 mm while the other one 0.9 mm. The strips are glued in two points on the tested object as to overlap each other.

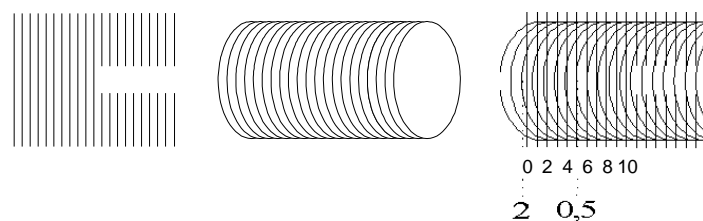


Fig. 5. Grid sensor designed for large strain measurements

The principle of the measurement is the same as with a slide caliper and the grid sensor does not reinforce the measurement area as it does with strain gauges.

Digital displacement caliper has two arms with small steel balls at their ends. During the measurement the balls are firmly pressed against conical pits in metal grips attached to the FST surface and the actual pits' distance can be read on the caliper display. The local strain measurements obtained with various tested methods were as follows:

- resistant strain gauge: 0.19
- specially designed strain gauge extensometer: 0.76 ± 0.02
- texture photography (diffraction method): 0.86 ± 0.25
- grid sensor: 0.94 ± 0.30
- digital displacement caliper: 1.2 ± 0.30

The reference strain values were the results obtained from the sample elongation measurement (grip distance)

$$\varepsilon = \frac{(257.9 - 256)}{256} = 0.74\%$$

and calculated from the known average stress and secant elasticity modulus

$$\varepsilon = \frac{\sigma}{E} = 0.84\%$$

A comparison of the two global reference and locally measured strains allows to choose the most suitable methods for FST tests. These are strain gauge extensometer and grid sensors. Digital displacement caliper was also qualified for further use as an additional method. The strain gauges were decided to be used in case of measurement on the belts which strengthen the gores' joints where lower strain can be expected due to the greater local stiffness of the FST walls. Measurement results obtained using the above four methods for the prototype FST are summarised in Table 1.

Table 1. Results of strain measurement on the prototype FST

Location	a	b	c	d	e	f	g	h	i	Comments
Sensor	Strain in %									
L1A	-2,1									Eight readouts, std. dev. $\sigma = \pm 2.8\%$
L2B				4,3						Eight readouts, std. dev. $\sigma = \pm 1\%$
T1		0,06								Wall not tensed
T2			5,5							Estimated on of the crack width basis

Location	a	b	c	d	e	f	g	h	i	
T3					1,94					Exceeds the measurement range
T4						2,64				Exceeds the measurement range
R1							5,3			
C1							5			
C2								3,7		
C3									2,7	
C4	0,6									

Measurement points are denoted with letters (a)...(i) and localised as follows:

- (a) upper surface of the air flange;
- (b) side wall of the tank just beneath the flange
- (c) strengthening around the outflow stub pipe near the glue joint
- (d) strengthening of the tank bottom and side wall joint
- (e) side wall near by the glue joint of two side wall gores and the tank bottom
- (f) strengthening of the glue joint of two side wall gores and the tank bottom
- (g) at the foot of the wall near the tank bottom
- (h) at the middle of the height of a side wall
- (i) side wall approx. 20 cm beneath the air flange

while sensors are denoted as: T1, T2, T3, T4 - strain gauge; L1A, L2B - digital caliper; R1 - grid sensor; C1, C2, C3, C4 - strain gauge extensometer.

Measurement locations (d), (g), (h) and (i) were at the same diagonal cross-section of FST. Eight of eleven results were qualified as being correct and these are marked in Table 1 with grey background colour. An important comment is that the result No.4 (strain gauge T2) is not the strain gauge readout. This strain gauge broke, as it is shown in Fig. 5, but was still fixed to the FST wall. The result 5.5% is an estimation on the basis of the crack width divided by the gauge dimension.

The conclusion was that the real strains are close to the estimated ones, so the application of strain gauges is not justified. On the other hand the simplest measurement method of the digital slide caliper has unacceptable standard deviation error (see Tab. 1) and the strain gauge extensometer was much more tedious in a field use then it had been expected. Results from the Table 1 are summarised in Fig. 6.

This preliminary experiment allowed to redesign the FST and to produce a final FST test copy (Fig. 3b) with the same storage volume (4000 m³) but greater diameter and lower height in order to improve its operational characteristic and decrease the circumferential strains.

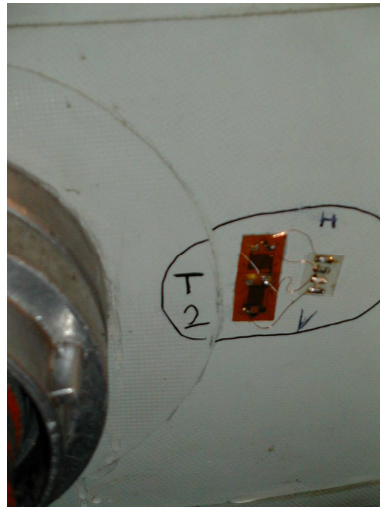


Fig. 6. Broken strain gauge T2

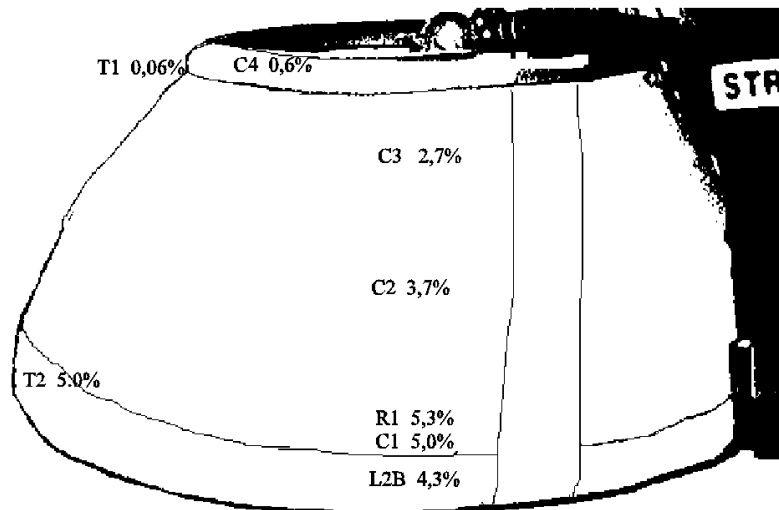


Fig. 7. Strains in the prototype FST

The new FST was tested under nominal load and the strains were measured with grid sensors only. The sensors were placed at five heights in two perpendicular cross-sections on both sides of the tank. There were used 40 grid sensors, 20 for vertical (diagonal) and 20 for horizontal (hoop) strain measurements. It was visible that the FST was not ideally levelled and its one side only was fully stretched and smooth. This side was called "high" while the opposite

side "low", and "left" and "right" sides in the perpendicular cross-section had the walls creased and not tensed beneath the flange. These four cross-sections were chosen for measurement purpose and vertical positions of the sensors in each cross-section were at $h_1 = 5$ cm, $h_2 = 23$ cm, $h_3 = 41$ cm, $h_4 = 59$ cm and $h_5 = 71.5$ cm beneath the flange (Fig. 8) [3].

Grid sensors were glued to the FST walls in its unloaded state and reference measurements were taken including the measurement of the active length of each sensor. After filling FST with water the other measurements were taken. In both cases the readouts were performed twice by two researchers. Taking into account the sensor resolution of 0.1 mm the readouts were in perfect agreement in every case. Then the measured displacement and calculated strains were compensated for the thermal shrinkage of the FST walls, as the filling water was 6°K cooler than the tank temperature while gluing the grid sensors. The compensated strains are given in Table 2 with additional comments regarding the local measurement conditions [4]. Analysis of individual results from Table 2 is not as the one for average values. It is worth to mention that "left" and "right" side measurements are much closer to each other in their values and tendency than those for "high" and "low" sides.



Fig. 8. Grid sensors glued to FST wall

This is consistent with expectations for such in situ experiments and confirms that local measurements should be taken in many points to yield general conclusions. The highest measured local strains are close to the estimated ones and are much lower than ultimate strains for TU - 08 material used for the FST manufacturing.

Table 2. Strains of the walls of a redesigned FST as measured with 40 grid sensors

	Sensor	Height beneath flange	Strain ‰	Average strain ‰	Comments
Horizontal (hoop) strains	H1h	-5 cm	0.0	x	
	H1lw		x		wall not tensed, creased
	H1r		x		wall not tensed, creased
	H1lt		x		wall not tensed, creased
	H2h	-23 cm	7.4	19.7	
	H2lw		x		wall not tensed, creased
	H2r		27.6		
	H2lt		24.1		
	H3h	-41 cm	8.0	26.0	
	H3lw		40.0		
	H3r		22.6		
	H3lt		33.3		
	H4h	-59 cm	9.4	33.5	
	H4lw		48.1		
	H4r		32.1		
	H4lt		44.4		
H5h	-71.5 cm	13.3	25.5		
H5lw		35.1			
H5r		25.0			
H5lt		28.6			
Vertical (diagonal) strains	V1h	-5 cm	31.1	x	
	V1lw		x		wall not tensed, creased
	V1r		x		wall not tensed, creased
	V1lt		x		wall not tensed, creased
	V2h	-23 cm	-3.9	0.5	
	V2lw		x		wall not tensed, creased
	V2r		20.3		
	V2lt		-14.8		
	V3h	-41 cm	-34.0	-0.9	
	V3lw		-10.5		
	V3r		37.0		
	V3lt		3.8		
	V4h	-59 cm	7.0	-0.8	
	V4lw		6.8		
	V4r		16.2		
	V4lt		-35.3		
V5h	-71.5 cm	40.7	48.7		
V5lw		60.4			
V5r		51.7			
V5lt		42.1			

Average hoop strains show almost linear increase with the height below the flange down to the bottom of FST where conical shape changes into a toroidal one. Although in this region there exists greater water pressure but there is a decrease

of the hoop strain. This is due to the strengthening of the wall by gluing together a side gore, a base gore and a belt.

This greater local stiffness does not stop an increase of average diagonal strain. These strains are close to zero on the side wall where there is no curvature of the wall in the gauge direction because of the conical shape of FST. But in the lower part of greater stiffness there arises a curvature in the diagonal cross-section which results in a high increasing of the vertical strain. Average strains are plotted in Fig. 9.

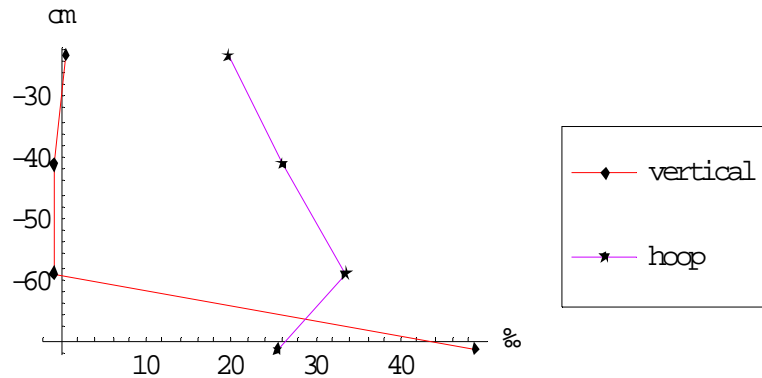


Fig. 9. Average hoop and diagonal strains from grid sensor measurements

4. Conclusions

There were developed strain measurement methods in walls of flexible self-supporting water tanks (FST) used in fire-extinguishing actions to protect buildings and other civil engineering structures.

Strain grid sensors developed for FST testing are a simple and effective measurement tool for large deformations and in situ test.

Strains of final test copy of FST are several times lower than the ultimate strains for TU - 08 material being used.

Maximal measured hoop and vertical strains are of the same order of magnitude which confirms the proper design of FST.

Developed measurement methods can be adapted for shell structures testing as well as other coverings made of technical fabrics.

5. Acknowledgement

Research was supported by State Committee for Scientific Research under Grant No. 148131/C-TOO/98.

BIBLIOGRAPHY

1. Z. Bednarek: Firefighting water tank with air-tight floating flange made of elastic technical fabrics. Final Report, Grant No. 148131/C-TOO/98 of State Committee for Scientific Research, The Main School of Fire Service, Warsaw, 2000 (in Polish).
2. M. Skłodowski: Research on development of methods and stand for testing firefighting water tanks made of elastic technical fabrics. *Techn. Rep. ZBS Epsilon*, Warszawa 1999 (in Polish).
3. M. Skłodowski, Z. Bednarek, E. Skłodowska: Testing method of self-supporting water tank with floating flange, presented at 19th DANUBIA-ADRIA Symposium on Experimental Methods in Solid Mechanics, Polanica Zdrój, POLAND, Sept. 25-28, 2002.